THE RICE INSTITUTE

14 - 18 MEV TOTAL NEUTRON CROSS SECTIONS OF H^1, H^2, Li^7, Be^9, B^{10} B^{11}, C^{12}, O^{16}, Mg, Al^{27}, and S^{32}

BY

CHARLES FALK COOK

A THESIS

SUBMITTED TO THE FACULTY

IN PARTIAL FULFILLMENT OF THE

REQUIREMENTS FOR THE DEGREE OF

DOCTOR OF PHILOSOPHY

HOUSTON, TEXAS

MAY, 1953

UMI Number: 3079655

UMI Microform 3079655

ProQuest Information and Learning Company
300 North Zeeb Road
P.O. Box 1346
Ann Arbor, MI 48106-1346

TABLE OF CONTENTS

I INTRODUCTION

Measurements of total neutron cross sections for nuclei using fast neutrons of various energies have been previously reported.[1-6] Several[1,2] of these used neutrons which were not monoenergetic. However, with the advent of monoenergetic neutrons from the reaction $T(d,n)He^4$, investigations have been reported giving total neutron cross sections at 14 Mev using monoenergetic neutrons in "good" geometry to various accuracies. Of these various reports, the data of Coon, Graves, and Barschall[5] point to deviations from the schematic theory of nuclear cross sections proposed by Feshbach and Weisskopf[7] for the lighter elements as well as some of the heavier elements. A systematic deviation from a plot of the equation

$$\sqrt{\frac{\sigma_T}{2\pi}} = k A^{\frac{1}{3}}$$

σ_T = total neutron cross section

A = atomic weight

was observed for the elements Be^9, B^{10}, B^{11}, and C^{12}. For these four elements the cross section was observed to be a decreasing function of the atomic weight. This effect is consistent with the data of Lasday[3] and Goodman[6] for Be^9 and C^{12}. Neither of the latter did the boron isotopes. The data of Lasday and Goodman also represents 14 Mev total neutron cross sections.

Of these investigations[1-6], no one group carried out cross section measurements at more than one particular neutron energy. It is of interest to see over what energy range these systematic deviations appear. The results of Cook, et al[8],

show that at 90 Mev the total neutron cross section for H, D, Li^7, Be^9, C^{12} are increasing with atomic weight. This indicates that at some point in the energy range 14 to 90 Mev these deviations disappear. The investigations carried out here are measurements of total neutron cross sections for some of tne light elements over the energy range 14 to 18 Mev.

In addition to checking for a systematic deviation similar to that found by Coon, et al[5], considerable attention was given to determination of the neutron-proton total cross section over the above energy range.

II EXPERIMENTAL PROCEDURE

1. Elements Investigated

The investigation carried out here involved the eleven elements shown in Table 1. The scatterers used were in cylinders of various diameters and lengths. The form or compound which was used for each element is also shown along with the diameters, lengths, and densities in Table 1.

Table 1

Element	Sample Form	Diameter inches	Length inches	Density gm/cm^3
H^1	CH_2	0.7463	0.4903	0.903
H^2	D_2O	0.7300	2.0000	1.00
Li^7	Metal	0.706	1.633	0.519
Be^9	Metal	0.6237	0.9993	1.82
B^{10}	Powder	0.7300	1.5000	1.26
B^{11}	Powder	0.7300	2.5000	0.557
C^{12}	Graphite	0.7518	1.5204	1.63
O^{16}	H_2O	0.7300	2.0000	1.00
$Mg^{24.3}$	Metal	0.7493	1.5078	1.79
Al^{27}	Metal	0.7501	1.5052	2.89
S^{32}	Cast	0.7500	1.5149	1.94

The purity of each sample varied and will be discussed in section III.

The lengths of the scatterers were chosen to give transmissions of 60 to 70%. This choice of transmissions kept the multiple scattering corrections negligible, and at the same

time permitted a sizeable difference in the counting rate with the scatterer in and the scatterer out of the neutron beam. The diameters of the scatterers were such that no neutrons entered the crystal that did not pass through the scatterer when in place.

The effect of the scattering of neutrons into the detector from the floor was checked by measuring the transmission of a five and one quarter inch copper rod. The floor effect was found to represent seven per cent transmission. This effect of the floor scattering neutrons into the detector would give a count in the detector whether the scatterer were in place or not. This would make the transmission measurement too high. The resulting cross section would then be too low. In as much that the chief concern here was the relative cross sections at the various energies, this correction was not applied to the data. The one correction applied to all of the data is discussed in section 3 of Experimental Procedure.

In the four cases where powders and fluids were used ten mil aluminum cylinders were used for holding the material. The transmissions of these aluminum cylinders were measured before filling with each material and were found to be 100% within the statistics taken in this experiment.

2. Description of Apparatus

The neutrons for this experiment were from the $T(d,n)He^4$ reaction. The target used was tritium absorbed in a thin layer of zirconium. The neutron energy was varied from 14.1 Mev to 18.0 Mev by variation of the incident deuteron

energy. The energy of the neutron as a function of the bombarding energy and the angle of emission with respect to the incident deuteron beam as measured in the laboratory system of coordinates is shown in Appendix 1.

A convenient arrangement to obtain 14.1 Mev neutrons from the deuteron-on-tritium reaction is to observe the neutrons at right angles to the incident deuteron beam as measured in the laboratory system. Such an experimental arrangement is shown in Figure 1 along with a block diagram of the electronics. The source of deuterons in this case was a 160 kev unresolved deuteron beam from the Rice Institute Cockroft-Walton accelerator. The major content of the beam was previously known to be molecular in nature. Monitoring of the neutron flux was accomplished by counting the associated alpha-particles from the reaction with a proportional counter at 90^{o} to the incident deuteron beam in the laboratory. The counter window was three-thirty-seconds of an inch in diameter which resulted in a solid angle of $4.09\ 10^{-4}$ ster-radians. The counter voltage was 1000 volts and the resulting pulse height distribution exhibited a plateau of some thirty volts.

An anthracene scintillator placed six inches from the neutron source was used as the neutron detector. The anthracene crystal was one inch long and three-quarters of an inch in diameter and was mounted on a 5819 photomultiplier. The bias voltage of the 5819 was approximately 750 volts. Pulses from the 5819 were fed directly to a cathode follower, to an Atomic Instrument Model 204B linear amplifier, to a Model

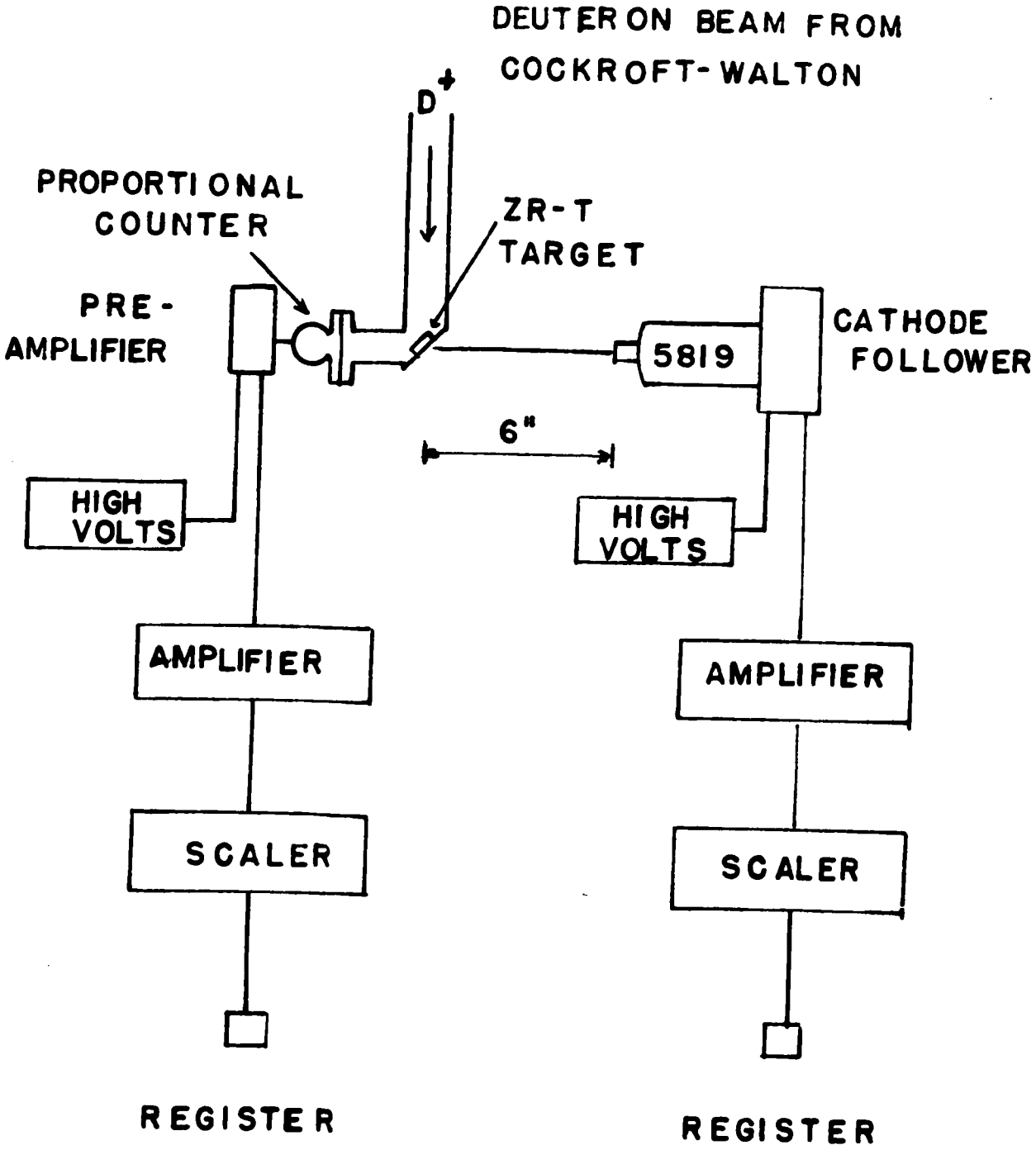
DEUTERON BEAM FROM
COCKROFT-WALTON
D+
PROPORTIONAL
COUNTER
ZR-T
TARGET
PRE-
AMPLIFIER
5819
CATHODE
FOLLOWER
6"
HIGH
VOLTS
HIGH
VOLTS
AMPLIFIER
AMPLIFIER
SCALER
SCALER
REGISTER
REGISTER

FIGURE 1

101 scaler and finally to a register. Pulses from the proportional counter were fed to a preamplifier and then to a similar amplifier, scaler, and register combination.

Higher energy neutrons were obtained by using the Rice Institute two Mev pressurized Van de Graaff accelerator as a source of deuterons. The deuteron beam was bent through a 90° magnetic analyzer so that the energy was defined to about ten kev. In order to obtain the highest energy neutrons available with this accelerator and to minimize the number of changes during the entire experiment, the neutron detector was placed at zero degrees to the incident deuteron beam. In place of the alpha-monitor used on the Cockroft-Walton accelerator, a second anthracene scintillator was used as a neutron monitor. The anthracene crystal was one-half inch in length and one and one-half inches in diameter and was mounted on a second 5819 photomultiplier. This monitor was placed eight inches from the target and at 90° to the incident deuteron beam. Since the 90° magnetic analyzer used here had a fringing field, it was necessary to provide magnetic shielding for the two photomultipliers. This was accomplished by using a mu metal shield surrounded by an iron shield one-thirty-seconds of an inch thick. The experimental arrangement used here is shown in Figure 2 with the block diagram of the electronics.

Whenever scintillation counters were used, a differential bias curve was run using the incident neutrons. The voltages of the 5819 and the gain of the amplifier were chosen so that the largest neutron pulses were approximately eighty

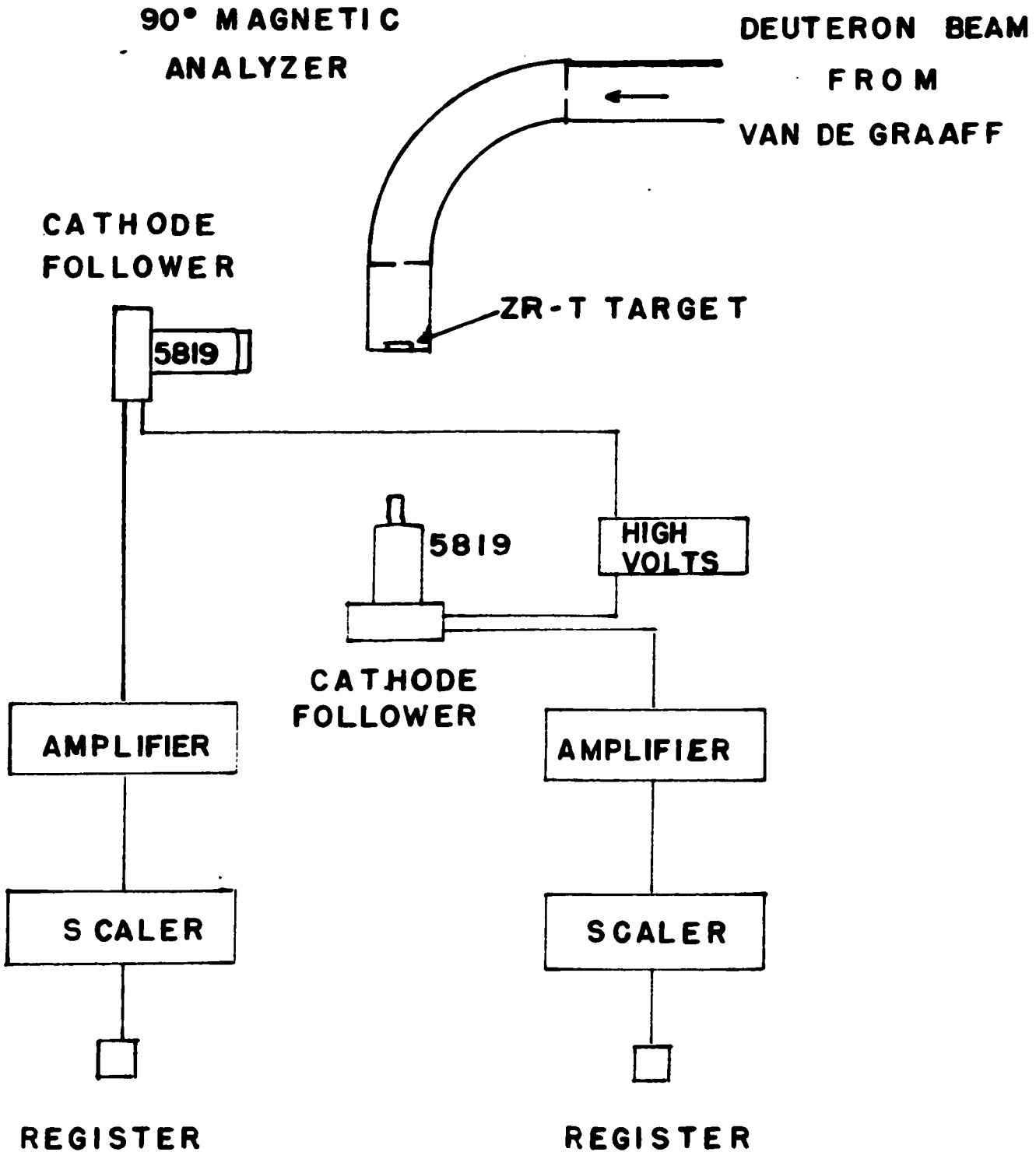
90° MAGNETIC
ANALYZER
DEUTERON BEAM
FROM
VAN DE GRAAFF
CATHODE
FOLLOWER
ZR-T TARGET
5819
5819
HIGH
VOLTS
CATHODE
FOLLOWER
AMPLIFIER
AMPLIFIER
SCALER
SCALER
REGISTER
REGISTER

FIGURE 2

volts. The scaler discriminator bias was set so as to be on the linear portion of the differential bias curve and in general counted only those neutrons which made pulses in the crystal of height greater than one-half the maximum pulse height. A typical bias setting with a cut off of eighty volts was forty-five volts. A setting such as this insured that the 3.1 Mev gamma radiation coming from the $C^{P}(d,p)C^{13}$ reaction was not counted.

A background count was interspaced throughout the taking of the data and at no time was it greater than 0.1% of the neutron counting rate in either crystal. In general, however, it was considerably less than 0.1%. The relative counting rates of the two crystals were adjusted so that the monitor crystal counted at approximately twice the rate of the neutron detector.

During the earlier runs a current integrator was used as an additional check on monitoring. No consistent difference was noted in the calculations of transmissions using the two different monitors. In some cases, which will be noted at the proper time, the current integrator was used as the monitor.

In both experimental arrangements shown in Figures 1 and 2 the front edge of the three-quarter inch diameter anthracene crystal was placed six inches from the Zr-T target. The scatterers were supported midway between the front edge of the crystal and the target by a thin brass support. This type of holder kept the unwanted scattering material in the neutron

beam to a minimum.

The apparatus was aligned by using an aluminum rod five and one-half inches long and three quarters of an inch in diameter. This aligning rod was placed in the thin brass support and the target, cylinder, and crystal were aligned by eyesight. No systematic deviations from day to day operation were observed that might be attributed to misalignment. The alignment was checked once before and once after each run. Those runs in which the alignment had changed were discarded. This misalignment also made itself known in the data by the presence of considerably higher transmission value for that particular run.

3. Measurements

In an experiment such as this, data is taken that enables the measurement of the total cross section from a knowledge of the experimentally determined transmission of neutrons through a scatterer of a given length. With either experimental arrangement as shown in Figures 1 or 2, the transmission of a beam of neutrons may be measured by taking a detector to monitor ratio with no scatterer in place and a similar ratio of detector to monitor with scatterer in place. Calling these R_1 and R_2 respectively, the transmission T is given:

$$T = \frac{R_2}{R_1}$$

From the transmission and a knowledge of the number of target

nuclei per cm^2, n, in the scatterer, the cross section, σ, may be determined from the following equation:

$$\sigma = -\frac{1}{n} \ln T$$

This formula however represents an idealized experiment, using a point source, point scatterer, and a point detector. Here we have none of these and inscattering corrections must be applied to the data taken. The inscattering corrections applied are those outlined by McMillan and Sewell[9] and for most scatterers amounted to about 10%.

The number of separate runs and total number of counts taken varied considerably from one sample to another as well as from one energy to another. However, all data was taken with counting statistics of one per cent or better. In the scatterers which could not be obtained in pure form, better statistics were required in order that the errors did not accumulate too rapidly due to subtraction.

A run consisted of four separate determinations of the transmission of a given scatterer. Counting statistics were in general 1% or better for each determination of scatterer in and scatterer out. The average of the four determinations represents one value of the transmission of a given sample at a given neutron energy. It was a general policy to run two scatterers alternately until a run on the two were completed. Particular attention was given to the pairing of the samples in some cases. The carbon and the paraffin were paired as were the heavy and ordinary water. The remainder of the samples were rotated in their pairings.

4. Neutron Energy Spread

Appendix 1 gives the formula for the calculation of the neutron energies as a function of the bombarding energy for the $T(d,n)He^4$ reaction. There are two sources of energy spread of the neutrons, namely the target thickness and the finite solid angle as seen by the neutron detector. Each of these will be discussed separately.

The target thickness was calculated using the stopping power of Zr as given by Warshaw.[10] The actual target thickness was 200 micrograms per cm^2. This resulted in an energy spread of at most 35 kev for a deuteron of the lowest energy used with this target. If the center of the target is to be considered as the average energy of the deuteron, the average correction in the energy of the deuteron should be about 18 kev. At the lowest deuteron energy used with this target, this energy spread in the target corresponds to an energy spread of 40 kev in neutron energy. At the highest deuteron energy the spread is reduced to about 20 kev.

For the calculation of the spread in neutron energy due to the finite solid angle subtended by the crystal, it is necessary to calculate the rate of change of neutron energy as a function of the angle of emission with respect to the incident deuteron beam. This is simply the derivative of the expression derived in the Appendix 1 and results in an expression as given below:

$$\frac{dE_n}{d\theta} = -\frac{2}{25} E_d \left[4\cos\theta\sin\theta + 2\sin\theta\, A(\theta) + 2\,\frac{\cos^2\theta\sin\theta}{A(\theta)} \right]$$

Since the angles involved are small, approximations may be used to determine the energy interval ΔE_n due to the finite angle $\Delta\theta$. This gives simply:

$$\Delta E_n = \Delta\theta \frac{dE_n}{d\theta} = -\frac{2}{25} E_d \Delta\theta \left[4\Delta\theta + 2\Delta\theta\, A(\Delta\theta) + \frac{2\Delta\theta}{A(\Delta\theta)} \right]$$

Shown in Table 2 are results of both of these calculations for the neutron energy spread. Column 1 gives the energy of the incident deuteron, column 2 gives the calculated neutron energy, column 3 the neutron energy spread due to target thickness, column 4 the neutron energy spread due to the finite solid angle, and column 5 the total spread in neutron energy.

Table 2

Deuteron Energy Mev	Neutron Energy Mev	Target Thickness Mev	ΔE_n Mev	Total Spread Neutron Energy Mev
0.190	15.08	0.040	0.009	0.049
0.333	15.43	0.037	0.011	0.048
0.596	16.09	0.035	0.017	0.050
0.870	16.58	0.032	0.021	0.053
1.200	17.09	0.029	0.026	0.055
1.500	17.51	0.025	0.029	0.054
1.780	18.00	0.021	0.032	0.053

III DISCUSSION OF RESULTS

1. Carbon and Hydrogen

In order that the neutron proton cross section be determined fairly accurately, a large number of runs was made on the carbon and the paraffin scatterers at each energy. The mean transmission at each energy, the standard deviation, and the number of runs for the carbon and paraffin scatterers are shown in Table 3. The calculation of the errors in the cross sections used the standard deviations given in Table 3. For carbon this is a straight forward process. However, since the calculation of the hydrogen cross section involves the subtraction of two separate cross sections, the manner used to calculate the error in the hydrogen cross section is outlined below.

Let T be the transmission and Δ T be the standard deviation given in Table 3. Also let σ be the cross section and ρ the number of atoms per square cm of the scatterer. There are two limits for the carbon cross section:

$$\sigma_{C+} = \frac{1}{\rho_C} \ln (T + \Delta T)_C$$

$$\sigma_{C-} = \frac{1}{\rho_C} \ln (T - \Delta T)_C$$

Likewise for paraffin:

$$\sigma_{CH_2+} = \frac{1}{\rho_{CH_2}} \ln (T + \Delta T)_{CH_2}$$

$$\sigma_{CH_2-} = \frac{1}{\rho_{CH_2}} \ln (T - \Delta T)_{CH_2}$$

Table 3

Neutron Energy Mev	Transmission Mean		Std. deviation		Number of Runs
	C	CH_2	C	CH_2	
14.1	.688	.689	.001	.002	13
15.0	.674	.693	.001	.001	13
15.5	.668	.693	.001	.002	12
16.0	.663	.703	.002	.002	17
16.5	.671	.702	.004	.004	7
17.0	.678	.704	.001	.002	4
17.5	.679	.710	.002	.004	6
18.0	.675	.717	.002	.004	8

From these four equations two extreme values for the hydrogen cross section may be calculated, namely:

$$\sigma_{H+} = \frac{1}{2}(\sigma_{CH_2^+} - \sigma_{C^-})$$

$$\sigma_{H-} = \frac{1}{2}(\sigma_{CH_2^-} - \sigma_{C^+})$$

The error in the hydrogen cross section used here is just:

$$\sigma_H \begin{matrix} + (\sigma_{H+} - \sigma_H) \\ - (\sigma_H - \sigma_{H-}) \end{matrix}$$

where σ_H is the hydrogen cross section determined from the mean carbon and paraffin transmissions at each energy.

In addition to the above data, some forty runs were made on the carbon scatterer alone over the energy range 15.8 to 17.0 Mev in approximately 40 kev neutron energy steps. A

different Zr-T target of deuteron thickness about 10 kev was used. The monitor used for this data was the current integrator rather than the anthracene monitor previously described. No sharp changes in the transmission were observed and the transmissions are shown in Figure 3. The plotted points represent the average of the runs at four energies and are plotted at the midpoint of the energy interval.

2. Oxygen and Deuterium

The cross section for oxygen was determined from the cross section of ten mil aluminum cylinder filled with ordinary water. The values for the hydrogen cross section used in the oxygen determination were those obtained for hydrogen discussed in the previous section. The oxygen cross section is given by:

$$\sigma_O = \sigma_{H_2O} - 2\sigma_H$$

The error in the cross section was determined in a manner similar to that described for the calculation of the hydrogen cross section in the previous section.

The cross section of deuterium was determined by comparing the transmissions of two identical ten mil aluminum cylinders, one filled with ordinary water and one filled with heavy water. The purity of the heavy water was known to be 99½%. No impurity corrections were applied. To check the identity of the two cylinders, each of the cylinders was filled with ordinary water and the transmissions were measured. The

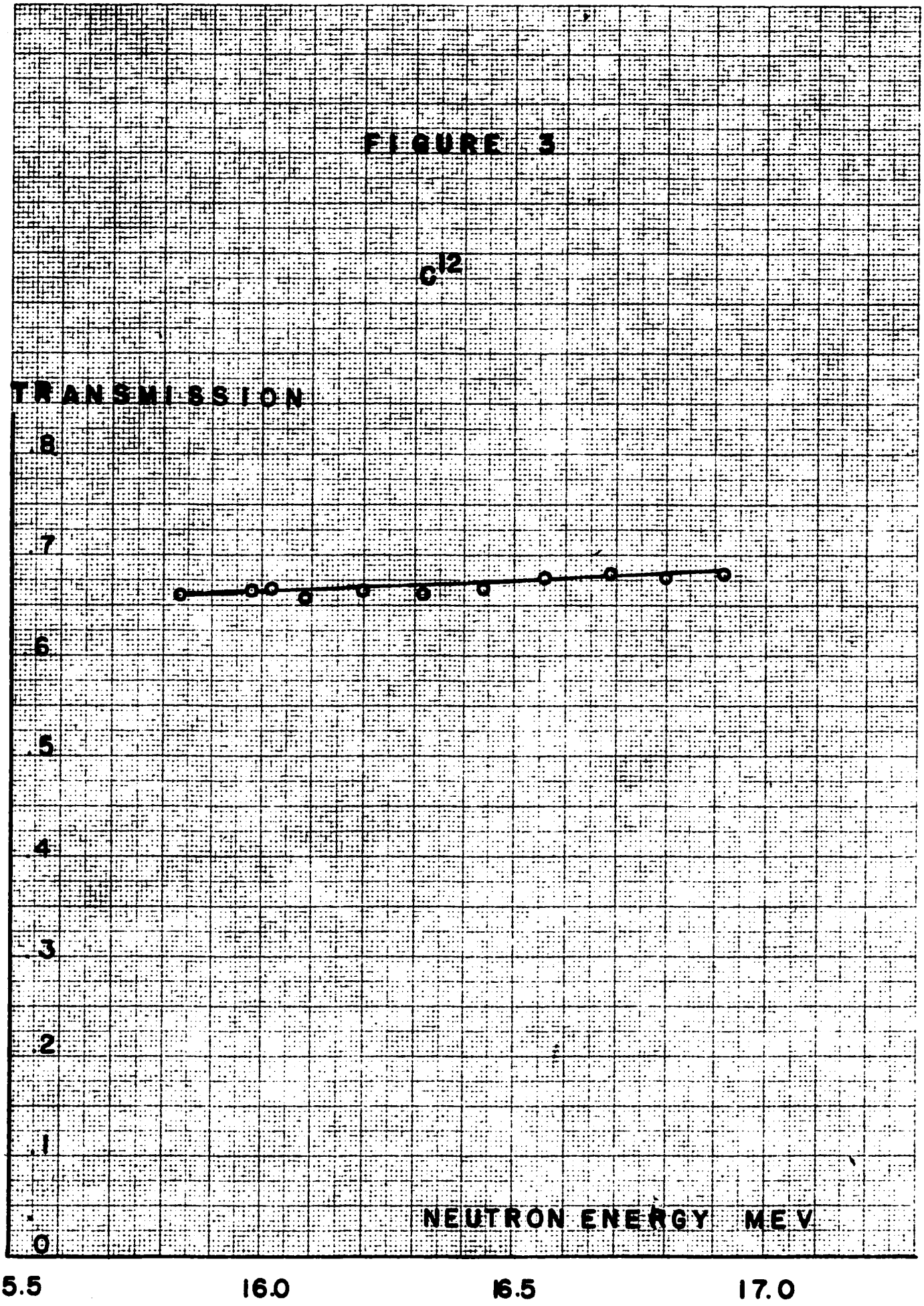
FIGURE 3
C12
TRANSMISSION
.8
.7
.6
.5
.4
.3
.2
.1
0
NEUTRON ENERGY MEV
15.5
16.0
16.5
17.0

transmissions of the two cylinders were identical within the statistics of this experiment.

If one assumes that there are the same number of atoms per square cm in both containers when filled with ordinary and heavy water respectively, it is easy to show that the deuterium cross section is given by:

$$\sigma_D = \sigma_H + \frac{1}{2\rho_{H_2O}} \ln \frac{T_{H_2O}}{T_{D_2O}}$$

The calculated error in the cross section was made as follows. Let T be the transmission and ΔT the standard deviation in the transmission, then the transmission ratio has two extreme values, namely a_+ and a_- given by:

$$a_+ = \frac{T_{D_2O} + \Delta T_{D_2O}}{T_{H_2O} - \Delta T_{H_2O}} \qquad a_- = \frac{T_{D_2O} - \Delta T_{D_2O}}{T_{H_2O} + \Delta T_{H_2O}}$$

The contribution to the error in the deuterium cross section would be given by the term:

$$\frac{1}{2\rho_{H_2O}} \ln \frac{a_+}{a_-}$$

This must be added to the error of the hydrogen to give the error in the deuterium cross section.

The neutron energies, mean transmissions, standard deviations, and number of runs for the ordinary and heavy water are given in Table 4.

Table 4

Neutron Energy Mev	Transmission Mean		Standard Deviation		Number of Runs
	H_2O	D_2O	H_2O	D_2O	
14.1	.622	.612	.002	.002	4
15.0	.626	.611	.002	.003	6
15.5	.633	.617	.003	.002	10
16.0	.658	.645	.005	.006	4
16.5	.644	.632	.003	.004	6
17.0	.653	.634	.006	.005	4
17.5	.650	.631	.004	.005	4
18.0	.652	.644	.003	.002	4

3. Lithium

The transmission of lithium was determined from a lithium cylinder enclosed in an air tight aluminum cylinder which contributed negligible scattering. The energies, transmissions, and standard deviations are given in Table 5. Only one run was made at each energy on the lithium cylinder. No impurity corrections were applied to the lithium cylinder.

Table 5

Neutron Energy Mev	Transmission	Standard Deviation
14.1	.780	.003
15.0	.787	.002
15.5	.786	.003
16.0	.798	.003
16.5	.805	.003
17.0	.803	.002
17.5	.810	.002
18.0	.831	.002

4. Beryllium

The transmission of beryllium was determined using a cylinder obtained from Brush Beryllium Company. The purity of sample was at least 98% beryllium, with at most 1½% beryllium oxide.

The remaining impurities were less than 0.1% each, the heaviest of which was iron. Since the corrections for the presence of the heavy impurities were probably less than ½%, their presence here was neglected. At most, the oxygen in the beryllium oxide could contribute about three quarters of one per cent to the cross section. Since the exact composition of the beryllium scatterer was not known, this correction was not applied. The transmissions and standard deviation of the beryllium scatterer of each energy are given in Table 6. Only one run was made at each energy.

An additional twenty two runs were made on the beryllium scatterer over the neutron energy range 15 to 16 Mev. The target used was the thin Zr-T target described previously in the discussion of the carbon scatterer. For these twenty two runs the current integrator was used as the monitor rather than the anthracene scintillator. No rapid changes in the transmission were observed. Figure 4 shows the average values of the transmissions for these runs.

Table 6

Neutron Energy Mev	Transmission	Standard Deviation
14.1	.655	.002
15.0	.659	.002
15.5	.669	.003
16.0	.663	.002
16.5	.662	.002
17.0	.669	.003
17.5	.677	.002
18.0	.678	.003

5. Boron 10 and Boron 11

The boron 10 used here was that supplied by the AEC. The composition of the enriched boron 10 supplied was stated as 98% boron (96% boron 10), 2% Fe, Mg, and Si. The ratio of the impurities is unknown. The average cross section for Fe, Mg, and Al at 14.1 Mev[5] was used for the impurity cross section

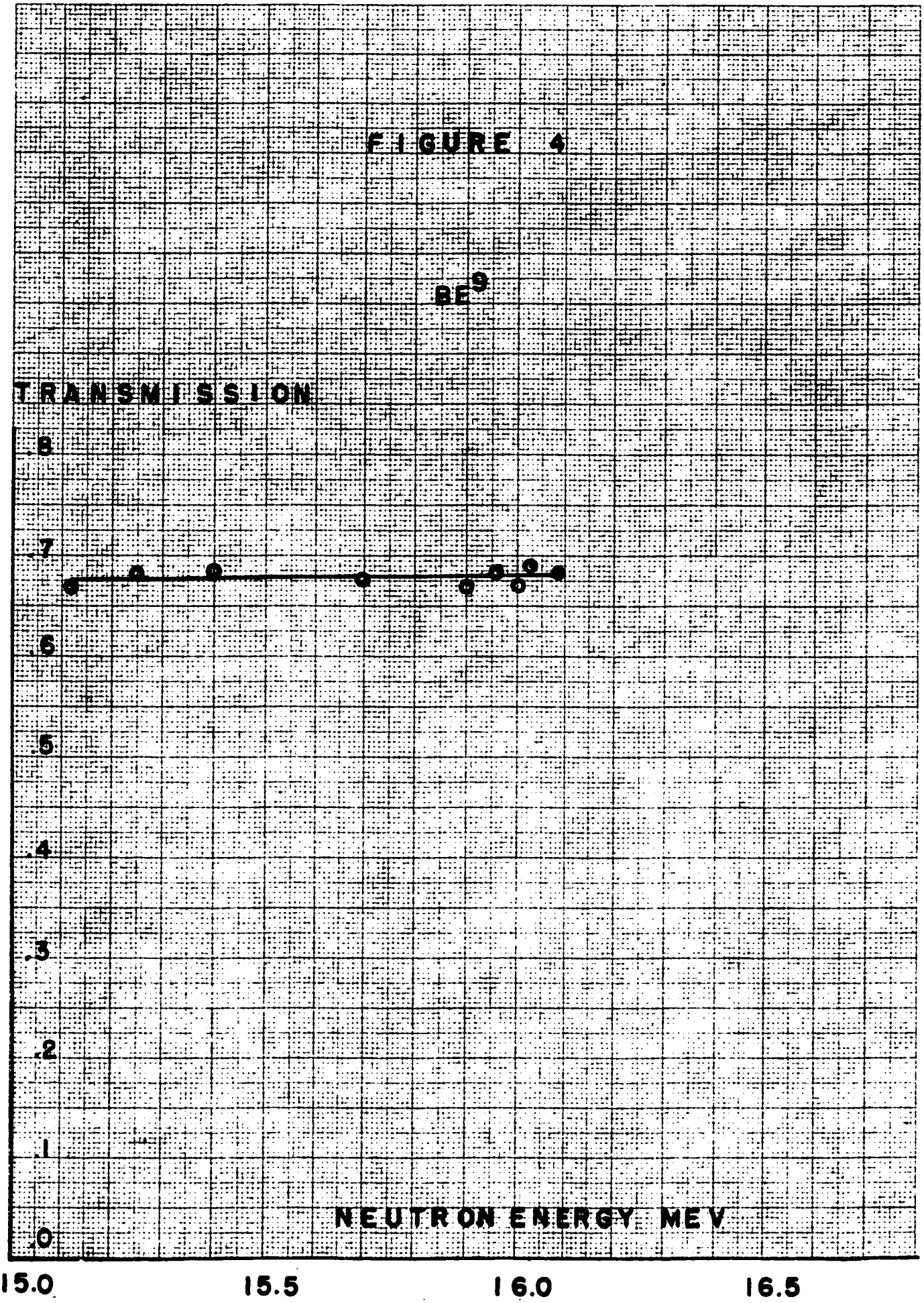
FIGURE 4
Be^9
TRANSMISSION
.8
.7
.6
.5
.4
.3
.2
.1
0
NEUTRON ENERGY MEV
15.0
15.5
16.0
16.5

value. The nuclear density of the impurity atoms was estimated from the average atomic weight of the three known impurities. This correction although calculated for 14.1 Mev cross sections, was applied over the entire range of energies in this investigation. A relation exists between the cross sections of the scattering cylinder, boron 10, boron 11 and the impurities.

$$.96\,\sigma_{B^{10}} = \sigma_{B^{10}_{cyl}} - \sigma_{imp} - .02\,\sigma_{B^{11}}$$

The boron 11 used was supplied by Fairmount Chemical Company with a stated purity of 99.2% and about a quarter per cent of Fe and C. These two impurities were neglected in the corrections. The atomic weight of the boron 11 was stated as 10.82. An equation may then be written giving the cross section relations of the boron cylinder, boron 10, and boron 11.

$$.82\,\sigma_{B^{11}} = \sigma_{B^{11}_{cyl}} - .18\,\sigma_{B^{10}}$$

The two equations may be used to determine the cross section of boron 10 and boron 11 from the transmissions of the two boron cylinders. The transmissions for the two cylinders are given in Table 7 with the standard deviations at each energy.

Table 7

Neutron Energy Mev	Transmission		Standard Deviation	
	B^{10}	B^{11}	B^{10}	B^{11}
14.1	.683	.750	.002	.002
15.0	.680	.750	.002	.003
15.5	.684	.748	.003	.002
16.0	.684	.747	.002	.003
16.5	.697	.753	.003	.003
17.0	.701	.753	.002	.003
17.5	.684	.766	.004	.003
18.0	.704	.772	.003	.003

6. Magnesium, Aluminum, and Sulphur

The impurities in these three scatterers, Mg, Al, and S, were unknown and no corrections were made for impurities. The counting statistics taken on these scatterers were only 2% at each energy. The current integrator was used as the monitor for the transmission data of Mg, Al, and S. No large changes in the transmission were observed in the transmissions for these three scatterers. The values for the cross section for these three elements are given in Table 8 for the various energies.

Table 8

Neutron Energy Mev	Cross sections Barns		
	Mg	Al	S
14.0	1.74	1.64	2.00
16.0	1.72	1.56	1.90
18.0	1.69	1.48	1.81

7. Discussion of Cross Sections

The values for the neutron cross sections as a function of the incident neutron energy for the various elements investigated are shown in Figure 5.

The slope of the cross section curves are approximately independent of the atomic weight over this energy range with the exeception of Li^7 and C^{12}. The cross section values themselves are in general decreasing and may with the exception of Li^7 and C^{12} be explained by the decrease in the neutron wavelength with increasing neutron energy.

The slope of the Li^7 cross section curve is approximately two and one-half times that of the other elements shown in Figure 5. There are several possible explanations.

1. If the radius of the Li^7 nucleus is very small the decrease in the neutron cross section due to the change in neutron wavelength with energy would be a greater effect for the Li^7 nucleus. However, even a very small radius will not allow the decrease in the neutron wavelength to account for the entire decrease in cross section over this energy range.

2. This rapid decrease in cross section may represent similar regularities as those observed by Barschall[12] in fast neutron cross sections for some of the medium nuclei with $100 < A < 140$. These scattering results carried out with neutron energies up to 3 Mev indicate that a single particle model is necessary for a theoretical explanation. Barschall's and his collaborator's results indicate that after averaging over the individual resonances the behavior of the cross section

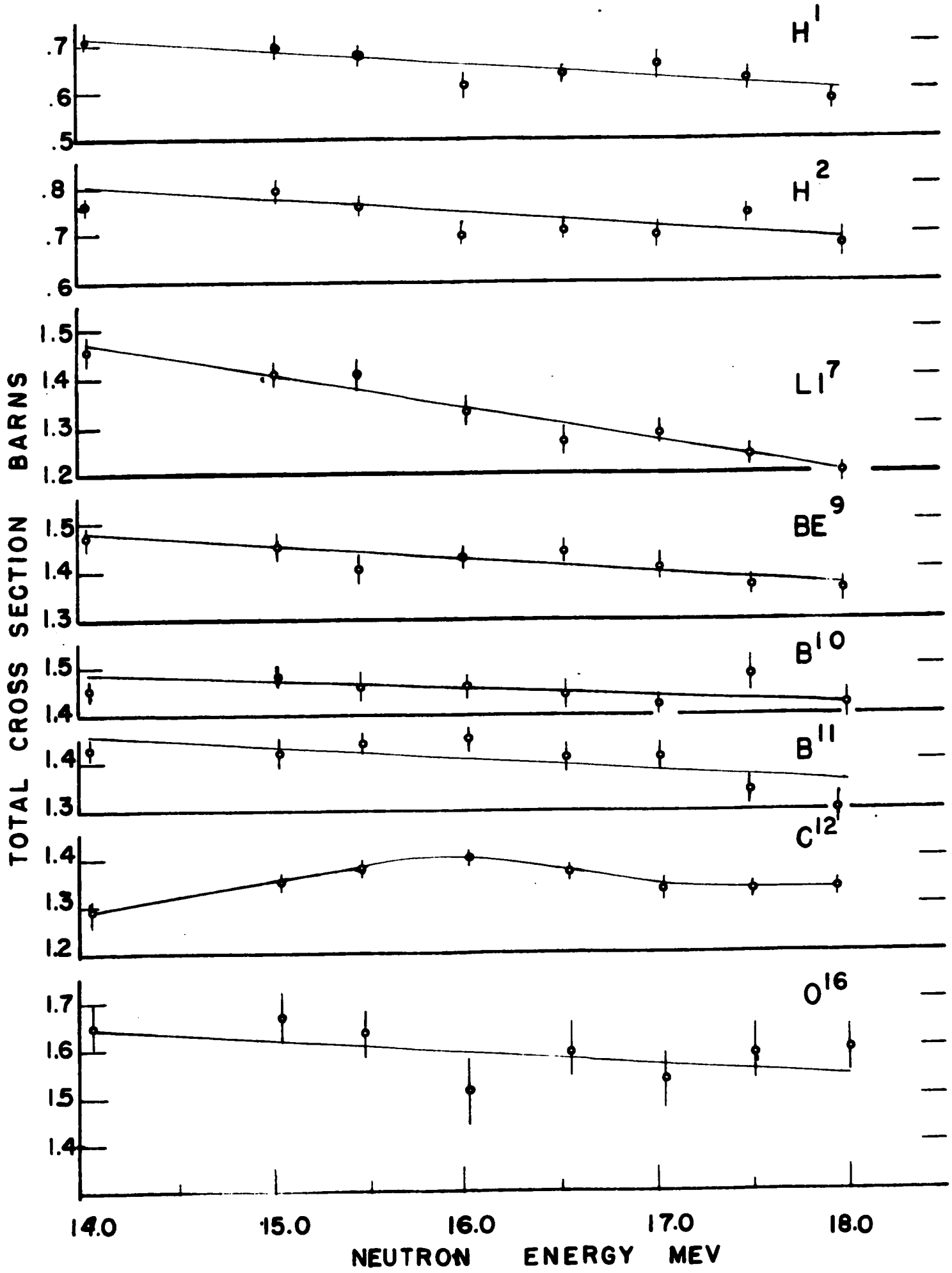
H1
H2
Li7
Be9
B10
B11
C12
O16
.7
.6
.5
.8
.7
.6
1.5
1.4
1.3
1.2
1.5
1.4
1.3
1.5
1.4
1.4
1.3
1.4
1.3
1.2
1.7
1.6
1.5
1.4
TOTAL CROSS SECTION BARNS
14.0
15.0
16.0
17.0
18.0
NEUTRON ENERGY MEV

curves is not smooth as predicted by the schematic theory, i.e., starting at $E^{-\frac{1}{2}}$ for low energies and reaching $2\pi R^2$ for high energies. Their experimental results show that at low energy the cross sections are low, increasing with energy to a wide broad maximum at about 1 Mev. This maximum seems to shift to higher energies with increasing atomic weight. Such a resonance has been shown by Weisskopf[13] to be predicted by the shell model using calculations of scattering by an independent particle from a potential trough the size of the nucleus and depth about 30 Mev. Unfortunately, however, several strong sharp resonances are predicted by this shell model calculation which were not observed by Barschall's group. It is possible then that the Li^7 nucleus has a broad maximum considerably higher than 1 Mev and that the decrease in cross section recorded here is the decrease due to this broad maximum occurring at somewhat lower energy than 14 Mev.

The beryllium cross section over the energy range 14 to 18 Mev is greater than the B^{11} and the C^{12} cross sections. However, the B^{10} cross section is equal to or greater than the beryllium cross section over this same energy range. These results indicate that the systematic deviations observed by the Los Alamos group for Be^9, B^{11}, and C^{12} are still present at 18 Mev. Within the limits of the experimental error, it is possible that the same deviations hold for Be^9 and B^{10}. In as much as the results at 14.1 Mev agree to within a few per cent of the data of the Los Alamos group,[5] deviations from the schematic theory of the nucleus as proposed by Feshbach and

Weisskopf[7] do occur in the 14 to 18 Mev energy range. A plot of the nuclear radii as a function of the cube root of the atomic weight is shown in Figure 6 for 14.1 Mev neutrons. These irregularities in the calculated nuclear radii of Be^9, B^{10}, B^{11}, and C^{12} led to the consideration of the average binding energies per particle for these nuclei. These energies are: Be^9 6.42 Mev , B^{10} 6.43 , B^{11} 6.88 , and C^{12} 7.64 . The greater the average binding energy per nucleon, the tighter binding in the nucleus. The consideration of these binding energies per nucleon might lead to a decrease in effective nuclear radii with increasing atomic weight for the above four elements.

It is noted from Figure 6 that the radius of the Li^7 nucleus is large for its atomic weight. This would possibly indicate a small average binding energy per nucleon. The average binding energy per particle for the Li^7 nucleus is only 5.57 Mev which is rather small.

Wilson[14] suggested a nuclear model in which the nucleon density is a constant out to the core radius R and then decreases as $e^{-\alpha r}/r^2$ where $\alpha^2 = \frac{2MW}{\hbar^2}$ and W is the binding energy per nucleon. Wilson's calculations show that the quantity $R + \frac{1}{\alpha}$ is more nearly the average nuclear radius. The values for R used by Wilson were calculated from the difference in Coulomb energies between an isobaric pair of atomic numbers Z and Z + 1, using known values of the end points of the positron spectra resulting from transitions between mirror nuclei. Wilson's calculations show an increasing average

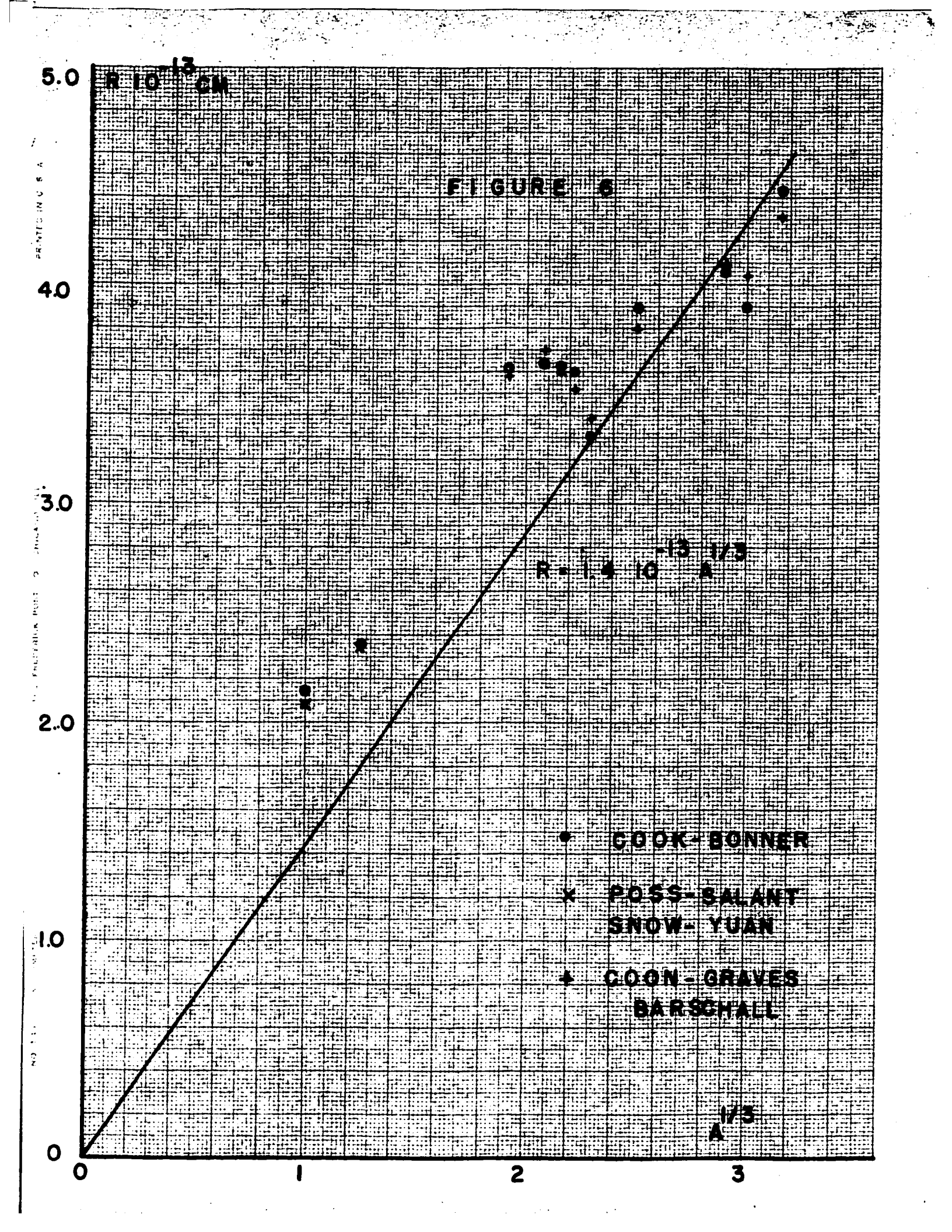
5.0
R 10^-13 CM
4.0
3.0
2.0
1.0
0
0
1
2
3
FIGURE 6
R = 1.4 10^-13 A^1/3
COOK-BONNER
POSS-SALANT
SNOW-YUAN
COON-GRAVES
BARSCHALL
A^1/3

nuclear radius, $R \neq \frac{1}{\alpha}$, with increasing atomic weight for the odd mass nuclei from A = 11 to A = 39.

Calculations of the average nuclear radius $R \neq \frac{1}{\alpha}$ for Be^9, B^{10}, B^{11}, and C^{12} have been carried out using the average value of R given by Wilson,

$$R = 1.1\ A^{1/3}\ 10^{-13}\ cm$$

These calculations failed to produce a decreasing average nuclear radius for increasing atomic weight for the above four elements. Table 9 shows the ratios of the nuclear radii of the elements to the radius of the Be^9 nucleus. Column 1 gives the element, column 2 the experimentally determined ratios at 14.1 Mev neutron energy, and column 3 the calculated average radius

Table 9

Element	$\frac{R_x}{R_{Be^9}}$	$\frac{R_x}{R_{Be^9}}$ calc.
Be^9	1.000	1.000
B^{10}	1.000	1.025
B^{11}	.988	1.038
C^{12}	.910	1.047

One further possibility is the introduction of a new constant into the schematic theory so the neutron cross section would be given by

$$\sigma = 2\pi k (R + \lambda)^2$$

The k in this equation must be a function of atomic weight as well as energy. Values for k have been obtained at two energies 14.1 and 16.0 Mev for each of the elements shown in Figure 5. These results are tabulated in Table 10. The general behavior of k seems to be strongly dependent on atomic weight. It is a decreasing function of atomic weight approaching unity slowly as the atomic weight increases. Nothing concrete may be said about the behavior of k with energy.

Table 10

Element	14.1 Mev	16.0 Mev
H	1.58	1.55
H^2	1.31	1.27
Li^7	1.46	1.28
Be^9	1.28	1.32
B^{10}	1.23	1.27
B^{11}	1.18	1.17
C^{12}	1.01	1.12
O^{16}	1.13	1.14

IV CONCLUSIONS

The total neutron cross sections for neutron energies from 14. to 18 Mev have been determined for H^1, H^2, Li^7, Be^9, B^{10}, B^{11}, C^{12}, O^{16}, Mg^{24}, Al^{27}, and S^{32}.

There is a broad resonance in C^{12} at 16 Mev neutron energy. It would be of interest to extend this investigation of the C^{12} cross section to higher neutron energies in search of other resonances that might occur.

The large slope of the cross section curve for Li^7 indicates the possibility of a neutron resonance at a lower energy than used here. Neutrons of energy up to 10 Mev may be obtained from $D(d,n)He^4$ reaction with deuteron energies available at Rice. Neutron energies from 12 to 14 Mev are available from the $T(d,n)He^4$ reaction. These two regions of neutron energies might yield some information on the possible neutron resonance mentioned above.

V APPENDIX

The kinematics of the $T(d,n)He^4$ reaction are exhibited here in a manner similar to that described by Hanson, Taschek and Williams.[8]

Let m_i, P_i, and E_i represent the mass, momentum and energy of the i th particle. Let Q be the reaction energy. Let the incident particle be i = 1, the target nucleus i = 2 with $E_2 = 0$, the neutron be i = 3 and the residual nucleus i = 4. Let θ_3 be angle of neutron emission with respect to incident particle i = 1 in lab system and θ_4 the angle of the residual nucleus as measured in the lab system.

The conservation of momentum gives:

$$P_4^2 = P_1^2 + P_3^2 - 2 P_1 P_3 \cos\theta_3$$

while the conservation of energy gives:

$$\frac{P_3^2}{2m_3} + \frac{P_4^2}{2m_4} = \frac{P_1^2}{2m_1} + Q$$

The energy of the residual nucleus i = 4 may be eliminated giving the neutron (i = 3) energy as a function of incident particle (i = 1) energy and angle of neutron emission θ_3.

$$E_3 = E_1 \frac{m_1 m_3}{(m_3+m_4)^2}\left\{2\cos^2\theta_3 + \frac{m_4(m_3+m_4)}{m_1 m_3} \times\left[\frac{Q}{E_1} + \left(1 - \frac{m_1}{m_4}\right)\right] \pm 2\cos\theta_3\left[\cos^2\theta_3 + \frac{m_4(m_3+m_4)}{m_1 m_3} \times\left[\frac{Q}{E_1} + \left(1 - \frac{m_1}{m_4}\right)\right]^{1/2}\right\}$$

For the $T(d,n)He^4$ reaction the above equation gives

$$E_n = \frac{2}{25} E_d \left\{ 2\cos^2\theta_3 + 10\left[\frac{17.58}{E_d} + \frac{1}{2}\right] + 2\cos\theta_3\left[\cos^2\theta_3 + 10\left[\frac{17.58}{E_d} + \frac{1}{2}\right]\right]^{\frac{1}{2}} \right\}$$

with a Q for the reaction of 17.58 Mev.

VI BIBLIOGRAPHY

1. Amaldi, Bacclavilli, Cacciapusti, and Trabacchi, Nuovo Cimento 3, 203 (1946).
2. R. Sherr, Phys. Rev. 68, 240 (1945).
3. A. H. Lasday, Phys. Rev. 81, 139 (1951).
4. Poss, Salant, Snow, and Yuan, Phys. Rev. 87, 11 (1952).
5. Coon, Graves, and Barschall, Phys. Rev. 88, 562 (1952).
6. Leonard S. Goodman, Phys. Rev. 88, 687 (1952).
7. Feshbach and Weisskopf, Phys. Rev. 76, 1550 (1949).
8. Cook, McMillan, Peterson and Sewell, Phys. Rev. 75, 7 (1949).
9. Edwin M. McMillan and Duane C. Sewell, U.S.A.E.C. Document MDDC - 1558.
10. S. D. Warshaw, Phys. Rev. 76, 1759 (1949).
11. Hanson, Taschek, and Williams, Revs. Mod. Phys. 21, 635 (1949).
12. H. H. Barschall, Phys. Rev., 86, 431 (1952).
13. V. F. Weisskopf, Physica. Deel XVIII, 12, 1083 (1952).
14. Robert R. Wilson, Phys. Rev., 88, 350 (1952).

ACKNOWLEDGEMENTS

The author wishes to express his appreciation to Dr. Bonner for his suggestion of the problem and his continued interest throughout the investigation. Also to extend appreciation to Mr. Van der Henst and the men of the shop for their assistance.